

The Preferred Conformation of the Tripeptide Ala-Phe-Ala in Water Is an Inverse γ -Turn: Implications for Protein Folding and Drug Design[†]

Andrea Motta,^{*,‡} Meital Rechtes,[§] Lucia Pappalardo,[‡] Giuseppina Andreotti,[‡] and Ehud Gazit^{*,§}

Istituto di Chimica Biomolecolare del CNR, Comprensorio Olivetti, Edificio A, Via Campi Flegrei 34, I-80078 Pozzuoli (Napoli), Italy, and Department of Molecular Microbiology and Biotechnology, George S. Wise Faculty of Life Sciences, Tel Aviv University, Tel Aviv 69978, Israel

Received April 11, 2005; Revised Manuscript Received August 28, 2005

ABSTRACT: Recent studies have provided evidence that peptides as short as tripeptides do adopt preferred conformations. Here we report that the tripeptide Ala-Phe-Ala (AFA) in aqueous solution preferentially forms an inverse γ -turn. Circular dichroism (CD) indicated the presence of a predominant turn structure, and Fourier transform infrared (FTIR) bands suggested the presence of a γ -turn forming a bifurcated H-bond with the solvent molecules. The high-resolution structure was obtained by a combined use of NMR spectroscopy and calculations. On the basis of 30 unambiguous ROESY-derived distance restraints (including the H α –NH NOE between Ala¹ and Ala³ and a hydrogen bond between the CO group of Ala¹ and the NH group of Ala³), calculations clearly demonstrated the presence of an inverse γ -turn centered on Phe². From NOE data, we estimated a mole fraction for the γ -turn of 0.65. Since for AFA an extended β -strand was also reported [Eker, F., Griebenow, K., Cao, X., Nafie, L. A., and Schweitzer-Stenner, R. (2004) *Proc. Natl. Acad. Sci. U.S.A.* 101, 10054–10059], we investigated the possibility that γ -turn and β -strand may represent two major conformations. By using a best-fit procedure that calculated experimental NOEs as weighted averages of the effects originating from both structures, we were able to calculate with good accuracy the backbone NOEs at 280 K in terms of the two limiting conformers, yielding a mole fraction for the γ -turn and β -strand conformations of 0.60 and 0.40, respectively, in good agreement with those found by NOE data. The implication of the existence of a preferred conformation by a small structural element is discussed in the context of the nucleation of protein folding events and the design of small peptide and peptidomimetic drugs.

The recent discovery that natural “disordered” (unfolded) proteins are endowed with very well-defined biological functions has suggested a reassessment of the structure–function paradigm (1, 2). Unfolded proteins and polypeptides are still considered completely unstructured because the ϕ and ψ dihedral angles are assumed to sample the entire allowed region of the Ramachandran space (3). This is somehow confirmed by early NMR experiments on short tri- and tetrapeptides in water, which found a random distribution of conformations.

Until recent years, there were only few studies that demonstrated a significantly preferential conformation of very short peptides. The most noted example was the YPGDV pentapeptide (4) that adopted ca. 50% β -turn conformation. Recently, multidimensional NMR has provided evidence that the conformational space of even tripeptides is more restricted than originally thought so that structures of limited stability can be formed. In this context, the polyproline II (PPII) conformation appears to be the most

relevant structural motif (5) even for non-proline residues in water (6, 7), therefore contrasting with the common belief that the structure of short peptides is random. A combination of Fourier transform infrared spectroscopy, polarized Raman spectroscopy, and vibrational CD measurements of several tripeptides suggested that trialanine and various alanine-based oligopeptides (8, 9) in water assume a temperature-dependent mixture of PPII and extended β -strand conformation, but even the Ala dipeptide seems to take up a predominantly PPII conformation (10). On the other hand, trivaline mostly adopts an extended β -sheet conformation (11). The pioneering work by the Schweitzer–Stenner group clearly established a new paradigm on the ability of short peptides to adopt preferential conformation; however, no direct high-resolution structure of a tripeptide in solution has been reported yet.

In our path for the study of the ability of very short aromatic peptides to form amyloid fibrils (12–14), we became interested in the structural features of the Ala-Phe-Ala (AFA) peptide. While it did not show any amyloidogenic potential, unlike similar short peptides with at least one aromatic side chain, AFA actually revealed a well-defined structure. Here we report that the preferred conformation of the tripeptide in water is an inverse γ -turn, with the formation of a possible bifurcated H-bond with the solvent molecules. From NOE data, we estimated a molar fraction for the γ -turn (x_{γ}^{NOE}) of 0.65. This appears to be an unusual finding as

[†] This work was supported in part by CNR/MIUR-Legge 449/97-DM 30/10/2000 (to A.M.) and the Bikura (FIRST) program of the Israel Science Foundation (to E.G.).

^{*} To whom correspondence should be addressed. A.M.: e-mail, amotta@icmib.na.cnr.it; phone, 39-081-8675-228/-226; fax, 39-081-8041-770. E.G.: e-mail, ehudga@tauex.tau.ac.il; phone, 972-3-640-9030; fax, 972-3-640-5448.

[‡] Istituto di Chimica Biomolecolare del CNR.

[§] Tel Aviv University.

γ -turns seldom exist in short, natural peptides, and may only be induced by α -aminoxy acid mimetics (15, and references therein).

Eker et al. (16) reported for AFA a β -strand-like conformation. Accordingly, we investigated the possibility that both the γ -turn and the β -strand-like conformations contribute to ROESY cross-peaks at 280 K, as they represent two major conformations that can be accessed by the tripeptide. By assuming the γ -turn and the β -strand as a basis set, we were able to simulate the NOE pattern via a best-fit procedure that calculated experimental NOEs as weighted averages of the effects originating from both structures. With this model, we calculated with good accuracy the backbone NOEs at 280 K, yielding for the γ -turn a mole fraction $x_{\gamma}^{\text{calcd}}$ of 0.60 and for the β -strand a mole fraction x_{β}^{calcd} of 0.40, with $x_{\gamma}^{\text{calcd}}$ very similar to x_{γ}^{NOE} found via NOE data.

A γ -turn is a type of reversed turn secondary structure that involves three amino acids forming a $3 \rightarrow 1$ hydrogen bond between the CO group of amino acid residue i and the NH group of amino acid residue $i + 2$. Depending on whether the side chain of residue $i + 1$ is in an equatorial or axial orientation on the pseudo-seven-membered ring, γ -turns are classified as inverse or classical, respectively (17, 18), giving rise to a kink in the chain or a direction change, respectively. γ -Turns, although less recurrent than β -turns, also play important biological functions. Structural studies have revealed that naturally occurring small peptides [namely, vasopressin (19) and the related desmopressin (20), bradykinin (21), and angiotensin II (22)] that function as hormones or neurotransmitters, or have other regulatory roles in organisms, adopt γ -turn conformations. The γ -turn present in the Arg-Gly-Asp sequence of vitronectin has been reported to contribute to the specific recognition by integrin receptor $\alpha_v\beta_3$ (23, 24), playing a role in tumor cell adhesion, angiogenesis, and osteoporosis. Finally, formation of hydrated reverse turns such as the one observed for AFA has been proposed to promote helix-coil unfolding (25).

MATERIALS AND METHODS

Circular Dichroism (CD) Spectroscopy. A stock solution of the peptide was prepared by dissolving AFA in double-distilled water to a concentration of 0.25 mg/mL, at acid, neutral, and alkaline pH. After a 5 min sonication, the peptide was diluted in double-distilled water in the experiment cuvette to a final concentration of 100 μ M. CD spectra were obtained using an AVIV 202 spectropolarimeter equipped with a temperature-controlled sample holder and a 5 mm path length cuvette. CD ellipticity, measured between 190 and 250 nm at 280 K, was averaged for 5 s.

Fourier Transform Infrared (FTIR) Spectroscopy. Infrared spectra were recorded using a Nicolet Nexus 470 FTIR spectrometer with a DTGS detector. AFA was dissolved in $^2\text{H}_2\text{O}$ to a final concentration of 0.25 mg/mL, at acid, neutral, and alkaline pH, and suspended on a CaF_2 plate. Measurements were taken by using a 4 cm^{-1} resolution and averaging 2000 scans. The transmittance minima were determined by the OMNIC analysis program (Nicolet).

NMR Data Collection. The peptide was dissolved in 0.5 mL of a $^1\text{H}_2\text{O}/^2\text{H}_2\text{O}$ mixture (90/10, v/v), and in $^2\text{H}_2\text{O}$ to yield concentrations in the range of 0.10–10 mM. The pH was adjusted to 1.2, 7.2, and 12.1 by adding HCl or NaOH

to obtain the cationic, zwitterionic, and anionic state of the peptide, respectively. Deuterated water was obtained from CortecNet.

NMR spectra, acquired at the NMR Service of Istituto di Chimica Biomolecolare del CNR (Pozzuoli, Italy), were recorded on a Bruker Avance 400 instrument, operating at 400.13 MHz, and a Bruker DRX-600 instrument operating at 600.13 MHz, using on both an inverse multinuclear probehead fitted with gradients along the X-, Y-, and Z-axes. In all spectra, quadrature detection in the t_1 dimension was accomplished using the hypercomplex method (26). Spectra were referenced to sodium 3-(trimethylsilyl)[2,2,3,3- $^2\text{H}_4$]-propionate. Homonuclear two-dimensional clean TOCSY (27) and ROESY (28) spectra were recorded by standard techniques and by incorporating the excitation sculpting sequence (29) for water suppression. We used a double-pulsed field gradient spin-echo with a soft square pulse of 4 ms at the water resonance frequency, with gradient pulses of 1 ms each in duration; 512 equally spaced evolution time period t_1 values were acquired, averaging four transients of 2048 points, with a spectral width of 6024 Hz. Time domain data matrices were all zero-filled to 4096 in both dimensions, yielding a digital resolution of 2.94 Hz/point. Prior to Fourier transformation, resolution enhancement was applied with a Lorentz–Gauss window to both t_1 and t_2 dimensions for all the experiments. ROESY spectra were obtained with a spin-lock field strength of 7 kHz and different mixing times (80, 120, 200, 300, and 400 ms) and temperatures (between 275 and 330 K); TOCSY experiments were recorded with a spin-lock period of 70 ms, achieved with the DIPSI-2 mixing sequence, at different temperatures to obtain the amide proton temperature dependence.

The natural abundance ^1H – ^{13}C HSQC spectrum (30) was recorded at 280 K at the pHs given above on the DRX-600 spectrometer operating at 150.90 MHz for ^{13}C ; 128 equally spaced evolution time period t_1 values were acquired, averaging 48 transients of 2048 points and using GARP4 for decoupling. The final data matrix was zero-filled to 4096 in both dimensions, and apodized before Fourier transformation by a shifted cosine window function in t_2 and in t_1 . Linear prediction was also applied to extend the data to twice its length in t_1 .

$^3J_{\text{NH}\alpha}$ and $^3J_{\alpha\beta}$ values were estimated in a double-quantum-filtered COSY spectrum in a $^1\text{H}_2\text{O}/^2\text{H}_2\text{O}$ mixture (90/10, v/v) (31).

Structure Determination. Distance restraints were obtained by integrating NOE peak volumes at different mixing times, and representing their buildup by a second-order polynomial. Assigned NOE cross-peaks, in the ROESY spectra with different mixing times, were volume-integrated by using a Monte Carlo approach (67), and interproton distances, d_{ij} , were calculated according to the relation

$$d_{ij} = d_{\text{ref}}(V_{\text{ref}}/V_{ij})^{1/6}$$

where d_{ref} stands for a known interproton distance between two protons and V_{ij} and V_{ref} stand for the integrated volumes of the i – j cross-peak and the reference cross-peak, respectively (32). As a reference distance, we used the two geminal methylene β -protons of Phe² separated by 0.178 nm.

ϕ and ψ dihedral angle restraints were derived from $^3J_{\text{NH}\alpha}$ coupling constants. The structure was calculated with 30

NOEs [14 intrasidue, 15 sequential ($\alpha\text{CH}_i\text{--NH}_{i+1}$, $\beta\text{CH}_i\text{--NH}_{i+1}$, and $\text{NH}_i\text{--NH}_{i+1}$), and one medium-range ($\alpha\text{CH Ala}^1\text{--NH Ala}^3$)]. Runs were first performed with distance restraints only.

Stereospecific assignments of Phe² side chain methylene H β 2 and H β 3 resonances were accomplished by qualitatively evaluating $^3J_{\alpha\beta}$ and NOE-derived distances using HABAS (33). For methyl groups, an additional correction of 0.03 nm was added for the highest apparent intensity of methyl resonances (34).

The structure was calculated with CYANA (35). A total of 100 randomized structures were generated, and the dynamics ran for 4000 and 35 000 steps (highsteps = 800 and 7000 and minsteps = 800 and 7000, respectively). The 10 structures with the lowest CYANA target functions, resulting from van der Waals and restraint violations, were chosen for further refinement. Energy minimization (EM) calculations were performed with GROMOS (36); bond length constraints were applied with the SHAKE method (37, 38). To release the strain caused by bad van der Waals contacts, while retaining the features of the original distance geometry structures, 800 steps of steepest descent restrained EM were applied. The list of nonbonded neighboring atom pairs was updated every 10 cycles of EM. A cutoff radius of 0.08 nm was used beyond which no nonbonded interactions were evaluated. Distance restraints obtained from NMR measurements were incorporated into calculations as a semiharmonic potential function with a force constant of 1000 kJ nm⁻² mol⁻¹.

The final structures were analyzed with the MOLMOL (39).

Energy Calculations. The united-atom (40) and all-atom (41) parametrizations of the AMBER force field were used in a series of EM calculations. The following steps were applied: (i) generation of starting models (vide infra), (ii) a united-atom EM calculation performed using a quasi-Newton method, the Broyden–Fletcher–Goldfarb–Shanno (BFGS) algorithm (42), stopping it when the gradient norm was $\leq 10^{-2}$, (iii) addition of nonpolar hydrogen atoms to the resulting structure, and all-atom BFGS EM run until a gradient norm of 10^{-3} was reached, and (iv) a final refinement obtained by a full Newton–Raphson minimization, with a convergence criterion on the gradient norm of $\leq 10^{-6}$. In the preliminary calculations, solvation effects were assessed by testing three different procedures on each conformation: (i) a distance-dependent dielectric constant $\epsilon = r$, (ii) a fixed $\epsilon = 10$ value, and (iii) a damped distance-dependent $\epsilon = 20r$. Apart from a general increase in the average hydrogen bond length between Ala¹ and Ala³, the folding patterns were essentially insensitive to ϵ variations, whereas side chains and terminal regions were affected to a larger extent. Since the experimental NOEs were measured in water at 280 K with a dielectric constant ϵ of ≈ 85 , we adopted the extreme solvation model by performing final refinements with an ϵ of $20r$.

RESULTS

CD Spectroscopy. The secondary structure of the AFA peptide in aqueous solution was initially investigated by CD spectroscopy. The CD spectrum at 280 K (Figure 1A) revealed a clear positive ellipticity in the far-UV region with

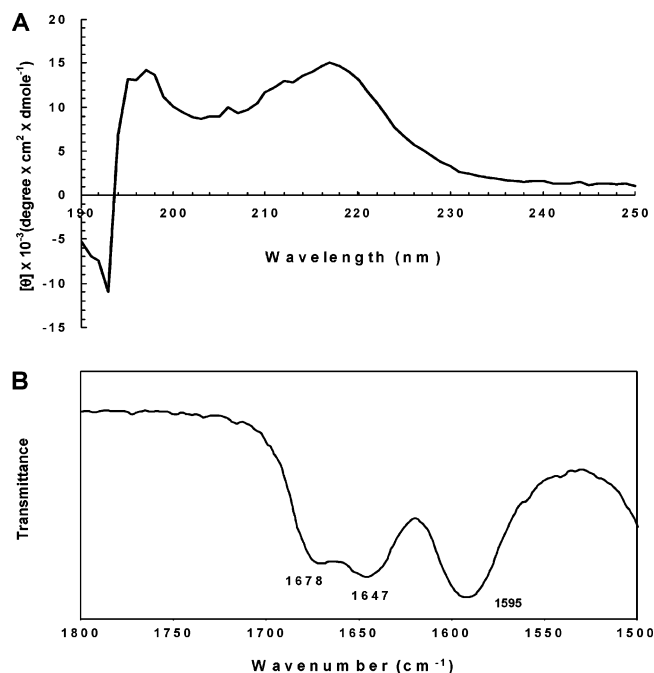


FIGURE 1: CD and FTIR spectra of AFA. (A) The circular dichroism spectrum was recorded at 280 K in 20 mM phosphate and 100 mM NaCl (pH 7.2) at a peptide concentration of 100 μM . (B) The Fourier transform infrared spectrum was recorded at 280 K at a peptide concentration of 0.25 mg/mL.

distinct double maxima at 197 and 217 nm, suggesting the presence of some turn structure. Identification of the nature of such nonrandom structure by CD is not possible due to the shortness of the peptide and the variety of CD spectra found experimentally for the different types of turns (43).

The AFA spectral features were retained after several days of incubation at high concentrations. Unlike the case with other short aromatic peptides, no signs of aggregation (see Aggregation State) or amyloid formation were observed upon ultrastructural analysis using electron microscopy (data not shown). The inability of the peptide to aggregate was further evidence of the presence of defined structure, different from a β -sheet that is a key for amyloid fibril formation.

FTIR Spectroscopy. Additional information about the AFA structure was obtained by FTIR spectroscopy in $^2\text{H}_2\text{O}$. Two minima were observed at the amide I region of the peptide spectra at room temperature (Figure 1B). The minima at 1678 and 1647 cm^{-1} are indeed consistent with the existence a predominant secondary structure, rather than a random conformation. A further band is observed at 1595 cm^{-1} . It has been reported that the bands at 1676, 1647, and 1595 cm^{-1} observed in the IR spectrum of cyclo[Pro-Ala-(CH₂)₅-CO] in $^2\text{H}_2\text{O}$ are indicative of the presence of an inverse γ -turn, with the low-wavenumber component band for a bifurcated (three-center) H-bond most likely involving solvent molecules (44). Water (or deuterated water) is reported to be easily involved in three-center H-bondings (45). Our FTIR band values correspond well to those for cyclo[Pro-Ala-(CH₂)₅-CO], therefore suggesting also for AFA an inverse γ -turn with a possible bifurcated H-bond with the solvent molecules.

It has been proposed that helix–coil unfolding is promoted by insertion of a water molecule into the α -helix $5 \rightarrow 1$ H-bonding via initial formation of a transient external or three-center H-bonding system (25). This leads to the

Table 1: ^1H and ^{13}C Chemical Shifts (parts per million) of AFA in a $^1\text{H}_2\text{O}/^2\text{H}_2\text{O}$ Mixture (90/10, v/v), at 0.10 mM, 280 K, and pH 7.2

residue	NH	C α H	C β H	others
Ala ¹	—	4.12	1.33	
		51.78	18.81	
Phe ²	7.78	4.63	3.23, pro-S	7.30 (C δ H), 7.38 (C ϵ H), 7.26 (C ζ H)
		56.22	2.99, pro-R	129.95 (C δ), 129.47 (C ϵ), 127.87 (C ζ)
			37.68	
Ala ³	7.32	3.80	1.40	
		49.99	17.64	

formation of a repertoire of hydrated reverse turns, like that found for AFA, connecting the α - and β -regions and so might facilitate the extremely rapid $\alpha \leftrightarrow \beta$ “flickering”.

Aggregation State. One-dimensional ^1H NMR spectra were recorded in aqueous solution at peptide concentrations in the range of 0.10–10 mM. We did not observe any appreciable change in either line widths or chemical shifts, each of which is suggestive of aggregation. Nevertheless, to check for the presence of aggregation at concentrations lower than those used in NMR experiments, fluorescence spectra were recorded for Phe². We found that the intensity of the Phe fluorescence emission at 282 nm (Phe excited at 257 nm) varied linearly with concentration up to 80 μM . As another test to rule out aggregation, CD spectra were acquired at peptide concentrations of 50 and 100 μM . Identical spectra were obtained at both concentrations, consistent with the absence of aggregation in this range (data not shown). Once the absence of aggregation over a wide range of peptide concentrations was confirmed, a peptide concentration of 0.10 mM was used in all the NMR experiments reported here.

NMR Analysis. ^1H NMR spectra of AFA in aqueous solution at various pH values and under denaturing conditions (8 M urea) were easily assigned using the standard sequential assignment procedure (46). The ^1H and ^{13}C chemical shifts are reported in Table 1.

The detection and identification of the folded conformations adopted by AFA were based on the structural information provided by ROESY data, H α conformational shifts (deviation of the chemical shift values with respect to those in completely unstructured peptides), and NH shift temperature coefficients (46). Figure 2 reports the ROESY spectrum of AFA recorded with a mixing time of 0.12 s at 280 K. Evidence for the presence of a chain bend in AFA comes from three points. First, there is the $\alpha\text{CH}_i\text{--NH}_{i+2}$ NOE between residues Ala¹ and Ala³ (labeled $1_\alpha\text{--}3_\text{N}$ in Figure 2). Second, the small temperature coefficient of the NH resonance of Ala³ (Table 2) indicates protection against solvent exchange by the possible involvement in an intramolecular hydrogen bond since for a tripeptide it is unlikely that a small value is due to the inaccessibility to the solvent. Third, are H α chemical shifts, whose deviations from unstructured (U) values are diagnostic of secondary structure. H α conformational shifts ($\Delta\delta = \delta - \delta_\text{U}$, in parts per million) are negative for helical or turn regions and positive in β -conformations or extended conformations (47).

Chemical shifts of H α protons of amino acid X in Gly-Gly-X-Ala tetrapeptides are frequently used as reference for the disordered state (48), but the H α chemical shifts for most peptides show small variations from these random coil

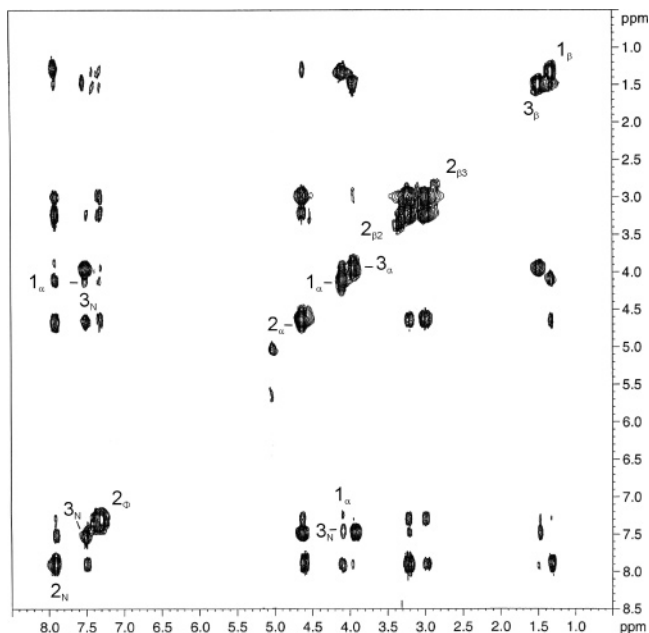


FIGURE 2: ROESY spectrum of AFA, acquired in a $^1\text{H}_2\text{O}/^2\text{H}_2\text{O}$ mixture (90/10, v/v), at 0.10 mM, 280 K, and pH 7.2, with a mixing time of 0.12 s. Peak labeling is reported along the diagonal. The NOE between the αCH group of Ala¹ and the NH group of Ala³, suggestive of the inverse γ -turn, is explicitly labeled.

Table 2: ^1H Coupling Constants (hertz) and Amide Proton Temperature Coefficients (parts per billion per kelvin) of AFA in a $^1\text{H}_2\text{O}/^2\text{H}_2\text{O}$ Mixture (90/10, v/v), at 0.10 mM, 280 K, and pH 7.2

residue	$^3J_{\text{NH}\alpha}$ (Hz)	$^3J_{\alpha\beta}$ (Hz)	$-\Delta\delta/\Delta T$ (ppb/K)
Ala ¹		7.2	
Phe ²	5.9	5.2	9.4
		9.2	
Ala ³	8.1	6.9	1.1

values. To avoid sequence effects on random coil δ values, the H α conformational shifts of AFA were evaluated using as a reference for the unstructured state H α chemical shifts obtained for the same peptide under fully denaturing conditions (8 M urea). This way of evaluating conformational shifts allows the detection of small populations of structure in partially folded peptides (49, 50). ROESY spectra of AFA in 8 M urea, performed to obtain the δ values under denaturing conditions, only contain sequential NOE connectivities less numerous and weaker (not shown) than those in an aqueous urea-free solution. Furthermore, the NH shift temperature coefficients of Phe² and Ala³ become ca. 10 ppb/K, suggesting exposure to solvent, the breaking of the intramolecular hydrogen bond, and therefore the disappearance of the turn under denaturing conditions. The H α conformational shifts with reference to 8 M urea are plotted as a function of the peptide sequence in Figure 3. The upfield αH chemical shift of Phe² of 0.19 ppm therefore indicates an α -conformation for this residue which is also in agreement with the small $^3J_{\text{NH}\alpha}$ value (Table 2).

AFA was studied at pH 7.2 in the zwitterionic state. Although the protonation state of the terminal groups has been reported to have only a very limited influence on the conformation of the central amino acid (51), we investigated AFA in the presence of NaCl, and at pH 1.2 (cationic state) and pH 12.1 (anionic state) to assess the effects of ion pair interaction on turn formation. ROESY spectra acquired in

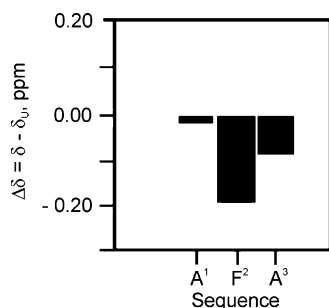


FIGURE 3: H α conformational shifts of AFA in a $^1\text{H}_2\text{O}/^2\text{H}_2\text{O}$ mixture (90/10, v/v), at 0.10 mM, 280 K, and pH 7.2. The H α conformational shifts were obtained with reference to 8 M urea under denaturing conditions ($\Delta\delta = \delta - \delta_U$, in parts per million), in aqueous solution at pH 7.2.

the presence of 10 mM to 1 M NaCl and at pH 1.2 and 12.1 did not significantly alter the NOE pattern, although a general resonance broadening was observed around 0.8 M NaCl. Taken together, these results show that the γ -turn observed for AFA at pH 7.2 cannot be attributed to ion pair interaction between charges on αNH_3^+ and αCOO^- groups in Ala¹ and Ala³, therefore confirming the limited influence of the charged terminal groups on the central residue (51).

Estimation of the γ -Turn Population. To estimate the population of the γ -turn formed by AFA, we used the ratio of the intensities of the H α –NH NOE between Ala¹ and Ala³, characteristic of the turn, to that of the H β –H β' Phe² NOE (intensity_{H α –NH} observed/intensity_{H β –H β'} Phe²), because being the H β –H β' Phe² distance constant, the H β –H β' Phe² NOE intensity can be used as a reference. The intensity ratio corresponding to 100% γ -turn was taken to be $(d_{\text{H}\alpha\text{--NH}_{i+2}})^{-6}/(d_{\text{H}\beta\text{--H}\beta'\text{Phe}^2})^{-6}$, where $d_{\text{H}\alpha\text{--NH}_{i+2}}$ is the distance between H α of the first residue and the NH group of the third residue found for the γ -turn in proteins (18, 52). This approach is clearly approximate, because it implicitly assumes equal correlation times for the peptide in any conformational state, and small variations in the actual H α –NH distance with respect to the averaged value in the γ -turn of proteins can lead to a large over- or underestimation of the turn population. Nevertheless, we believe that this approach safely estimates turn population (53). Accordingly, from NOE data, we estimated for the inverse γ -turn a molar fraction x_γ^{NOE} of 0.65, most likely interconverting with other conformations, including those corresponding to the “unfolded state”. This term implies that there are no strongly preferred backbone conformations, with small energy differences existing among different backbone conformations, namely, on the order of kT (54). When the energy differences among backbone conformations are large compared with kT , there will be one strongly preferred backbone conformation (54).

As a comparison, the γ -turn population was also estimated by using the H α conformational shift, obtaining a molar fraction $x_\gamma^{\Delta\delta\text{H}\alpha}$ of 0.58. By following Santiveri et al. (55, and references therein), we also used $^{13}\text{C}_\alpha$ and $^{13}\text{C}_\beta$ conformational shifts. From $\Delta\delta^{13}\text{C}_\alpha$ and $\Delta\delta^{13}\text{C}_\beta$, we obtained the following: $x_\gamma^{\Delta\delta^{13}\text{C}_\alpha} = 0.55$ and $x_\gamma^{\Delta\delta^{13}\text{C}_\beta} = 0.52$, respectively. The discrepancy between an x_γ^{NOE} of 0.65 (obtained from NOE data) and an x_γ^{calcd} of 0.60 (obtained from the best-fit procedure; see below) could be due to Phe² aromatic ring current effects on H α chemical shifts, and conformational flexibility affecting $^{13}\text{C}_\alpha$ and $^{13}\text{C}_\beta$ chemical shifts through ϕ

Table 3: Structural Statistics for the Bundle of 10 Selected AFA Structures

no. of experimental restraints	
intrareidue NOEs	14
interresidue sequential NOEs ($ i - j = 1$)	15
interresidue medium-range NOEs ($1 < i - j \leq 3$)	1
total NOEs	30
hydrogen bond restraints	1
total restraints	31
restraint violations ^a	
NOE distances with violations of >0.01 nm	5 ± 2
NOE distances with violations of >0.02 nm	1 ± 1
NOE distances with violations of >0.03 nm	0.4 ± 0.4
rmsd from the average structure	
backbone atoms (nm)	0.040 ± 0.0036
heavy atoms (nm)	0.22 ± 0.024
ϕ and ψ rmsd from average values (deg)	16.71
for the whole chain	
angular order parameter S^b for the whole chain	0.918

^a No restraint violation larger than 0.032 nm was detected. ^b From ref 68.

and ψ backbone dihedral angles (55, and references therein). Nonetheless, all the population values fall in a narrow range, and indicate that a consistent percentage of AFA takes up a γ -turn.

AFA Three-Dimensional Structure in Aqueous Solution. For a peptide as small as AFA, NOE intensities cannot be rigorously interpreted in terms of a unique structure due to the usual conformational averaging. Nevertheless, it is useful to calculate a limited number of structures compatible with NOE constraints, which help to visualize the conformational properties of the ensemble, albeit in a very simplified way. Structure calculations were performed on the basis of the complete set of NOE-derived distance restraints obtained for AFA in aqueous solution at pH 7.2, and using a distance geometry procedure (35). Starting from 100 randomized conformations, we selected 10 conformers that satisfy the constraints with no violation greater than 0.013 nm. The value of the pairwise root-mean-square deviation (rmsd) for the backbone atoms of the 10 conformers was 0.040 ± 0.0036 nm, while for all heavy atoms, it was 0.22 ± 0.024 nm. The structures calculated without any angle constraint were less well defined (rmsd for the backbone atoms and all heavy atoms of 0.21 ± 0.018 and 0.47 ± 0.061 nm, respectively). For Phe², the experimental average ϕ and ψ were $-91 \pm 18.2^\circ$ and $60 \pm 15.3^\circ$, respectively, which fit an inverse γ -turn centered on Phe². Furthermore, all of the calculated structures presented a hydrogen bond between the CO group of Ala¹ and the NH group of Ala³, with a hydrogen-acceptor distance of 0.24 nm and a relative frequency of 94%. The structural statistics of the 10 NMR structures are summarized in Table 3, while a representative low-energy structure of AFA is shown in Figure 4.

By a combination of vibrational spectroscopic techniques, Eker et al. (16) reported for AFA a mostly extended, β -strand-like conformation at higher temperatures. Furthermore, analysis of the ROESY spectrum in Figure 2 shows the contemporary presence of strong sequential $\alpha\text{CH}_i\text{--NH}_{i+1}$ effects, typical of extended structures, and an $\text{NH}_i\text{--NH}_{i+1}$ effect, typical of folded structures. Accordingly, we investigated the possibility that the γ -turn and the β -strand-like conformations coexisted at 280 K and represented two major conformations that can be accessed by the tripeptide. The change from the γ -turn to the β -strand was evaluated by

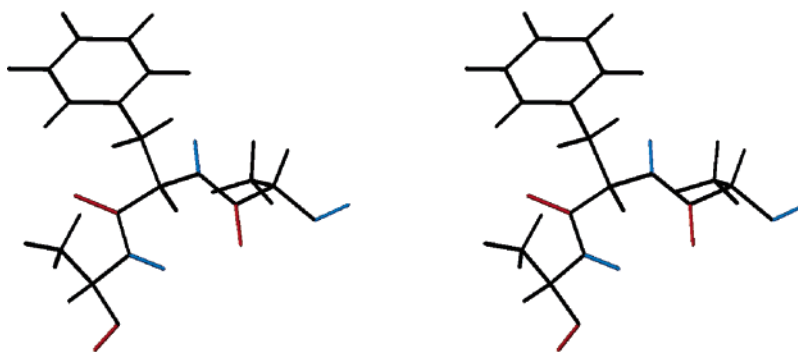


FIGURE 4: Inverse γ -turn of AFA. Stereoplot of a representative structure of AFA as obtained from NMR-derived restraints.

monitoring the dependence of the diagnostic Ala¹–Ala³ NOE intensity on temperature. In the range of 275–330 K, ROESY spectra of AFA showed a regular decrease in the magnitude of the NOE as the temperature was increased, with a plateau at ca. 280 K (not shown). On the other hand, a temperature increase did not alter the remaining NOE pattern, showing strong sequential NOEs that indicated the evolution of the peptide structure toward an extended form (46). According to these results and depending on temperature, the AFA predominant structure appears to be the γ -turn at low temperatures and the β -strand at high temperatures. The question of whether using both structures satisfies the observed NOE pattern better arises, since the NOEs most likely contain a contribution from both structures. The NOE pattern was fit by “separating” contributions from each structure via a best-fit procedure that calculated NOEs as weighted averages of the effects originating from γ -turn and β -strand. Accordingly, we tried to reproduce observed NOEs by using the minimum possible number of conformations as a basis set (56). We chose to start from several folded conformations to minimize the danger of local minima. The NMR analysis given above indicates that a reasonable starting conformation for AFA in internal energy calculations was the inverse γ -turn. Other starting structures were the classical γ -turn, and PPII found for other AXA tripeptides (16). Several runs of simulated annealing were also performed to find additional unbiased structures. Energy calculations were based on the united (40) and all-atom (41) parametrizations of the AMBER force field (see Materials and Methods). To account for solvation effects in an environment with a high dielectric constant, calculations were performed with dielectric constants whose actual value is a damped function of interatomic distances (see Materials and Methods). The results of this conformational analysis can be summarized as follows. The AFA refined structure is characterized by internal coordinates consistent with the inverse γ -turn family suggested by NMR (Figure 4). A hydrogen bond, characterized by a H–O distance on the order of 0.2 nm, was observed between the CO group of Ala¹ and the NH group of Ala³, while no salt bridge between peptide termini was observed. The structures obtained from a classical γ -turn and a PPII are less stable than the inverse γ -turn by ca. 50 kJ/mol. In fact, the latter is able to “survive” through changes of ϵ better than all other structures (including those derived from simulated annealing); that is, although it is not the absolute minimum when $\epsilon = r$, it is one of the lowest-energy structures and becomes the absolute minimum when $\epsilon = 20r$.

Table 4: Relevant Internal Coordinates of the Molecular Models of AFA Used in the Calculations of Experimental NOEs in a ¹H₂O/²H₂O Mixture (90/10, v/v), at 0.10 mM, 280 K, and pH 7.2

	γ -turn conformer				β -strand conformer			
	ϕ (deg)	ψ (deg)	χ_1 (deg)	χ_2 (deg)	ϕ (deg)	ψ (deg)	χ_1 (deg)	χ_2 (deg)
Ala ¹		142.5				151.4		
Phe ²	−88.8	68.2	−59.4	100.8	−146.7	164.6	−63.8	104.4
Ala ³	−142.4	146.7			−137.4	139.2		

The extended conformer was built on dihedral angles reported by Eker et al. (16) for AFA ($\phi = -140 \pm 15^\circ$, and $\psi = 170 \pm 10^\circ$) and served as input of an internal EM for which $\epsilon = 20r$. This conformer is less stable than the turn by ca. 23 kJ/mol. Simulation of experimental NOEs was performed with a continuous variation of the concentrations of the two limiting structures, and the best fit was obtained with $x_{\gamma}^{\text{calcd}}$ of 0.60 and an x_{β}^{calcd} of 0.40, corresponding to mole fractions of the γ -turn and β -strand conformers, respectively. It is worth noting that none of the “non-observed” NOEs has a counterpart in calculated NOEs larger than 1%, and such a “negative” result lends support to the fitting procedure of the experimental NOEs of AFA in terms of γ -turn and β -strand structures. The final internal coordinates of the turn and strand conformers used in the simulation of the NOEs are reported in Table 4.

DISCUSSION

The notion that peptides as short as tripeptides may adopt a stable conformation in an aqueous solution has been put forward in recent years (16, 51, 57). Several spectroscopic techniques indicated that peptides might exist in a predominant fold rather than as random structures. Here we provided a detailed structural analysis of AFA in water, based on NMR and calculations, showing the existence of a confined family of minimal energy structures all adopting an inverse γ -turn. Furthermore, FTIR spectroscopy suggested the presence of a bifurcated (three-center) H-bond most likely involving solvent molecules. In aprotic solvents (anhydrous DMSO and TFE) (data not shown), the NOE between Ala¹ H α and Ala³ NH, suggestive of the inverse γ -turn, was not observed in ROESY spectra of AFA. This suggests that the tripeptide does require water as a solvent for the formation of the inverse γ -turn, which disappears in a nonaqueous environment. It is tempting to speculate that formation of the hydrated bifurcated H-bond is functional to the γ -turn. This finding is of particular biological relevance in that hydrated reverse turns have been suggested to promote helix–coil

unfolding by facilitating the extremely rapid $\alpha \leftrightarrow \beta$ flickering (25, 58).

By a different experimental approach, a combination of vibrational spectroscopic techniques, Eker et al. (16) indicated a different conformation for AFA, a mostly extended, β -strand-like conformation, even at high temperatures. This discrepancy could be linked to the different time scales investigated by the two approaches, and/or to different temperatures. However, they could also represent two major conformations that can be accessed by the tripeptide. We found that, depending on temperature, the inverse γ -turn and the β -strand are predominant structures at low and high temperatures, respectively, and that the two families, although with different percentages, coexist as suggested by the NOE pattern observed at 280 K. Starting from selected conformations, we were able to separate each contribution via a best-fit procedure, and to calculate NOEs as weighted averages of the effects originating from γ -turn and β -strand. This conformational analysis suggests that the refined structure of the folded conformer of AFA is characterized by internal coordinates consistent with the family structure suggested by NMR (Figure 4). By continuous variation of the concentrations of the two limiting structures, the best fit was obtained with an $x_{\gamma}^{\text{calcd}}$ of 0.60 and an x_{β}^{calcd} of 0.40, corresponding to mole fractions of the γ -turn and β -strand conformers, respectively, which parallel the x_{γ}^{NOE} of 0.65 found from NOE data. Although a model relying on inverse γ -turn and β -strand structures is certainly not exhaustive, none of the nonobserved NOEs has a counterpart in calculated NOEs larger than 1%, therefore suggesting the absence of other significant structures.

Milner-White (18) has suggested that inverse γ -turns may function as intermediates in folding that help stabilize β -strands before they become β -sheets. Our data seem to support Milner-White's suggestion, indicating that temperature is a way to regulate the transition between γ -turn and β -strand structures.

Our results do not support the notion that small peptides exhibit infinite conformational flexibility. On the other hand, they provide evidence that tripeptides can adopt a well-defined structure in solution, which is not stabilized by electrostatic interactions between the terminal groups. This suggests that, as pointed out by Zimmermann and Scheraga (59), local interactions are strong enough to give rise to structure propensities of small peptide fragments and the unfolded state of proteins. That fits nicely into the picture emerging from investigations on longer alanine-based peptides (8, 9).

The observed γ -turn conformation may indeed provide a new insight into the study of protein folding. It has previously been suggested that reverse turns play a key role in the initiation of protein folding (59, 60). Stable turn conformations adopted by a domain of a polypeptide chain significantly restrict the conformational space that is available for the folding peptide chain. These results in bringing distant parts of the peptide chain into spatial proximity may facilitate long-range interactions, such as H-bonds, aromatic interactions, and electrostatic interactions. Indeed, mutations within proteins that disrupted local turn conformations resulted in protein misfolding (60, 61).

γ -Turns are often situated in the middle of β -sheet strands, and they have the effect of enhancing the pleated nature of

the sheets by inserting a kink in the polypeptide chain. Consecutive γ -turns generate a specific H-bond arrangement, called a "compound γ -turn", which could help stabilize individual β -strands before they associate to form a sheet (18). Therefore, (de)stabilizing β -strands through γ -turns could be a way of modulating β -sheet-driven amyloidogenesis.

Tripeptides are biomedically relevant as protease inhibitors (62), as taste receptors (63), and for enzyme regulation (64), and maintenance of a stable γ -turn conformation in a small drug may be critical for the attainment of activity (65, 66). The AFA and other stable tripeptides may serve as a model as well as a molecular scaffold for future drug design. Understanding the molecular basis of the structural features of small tripeptides may be useful for the design of small bioactive peptides with the low-molecular mass constrain (<500 Da) that is consistent with typical small molecule oral bioavailable drugs.

ACKNOWLEDGMENT

We thank Prof. Shmuel Carmeli (Tel Aviv University) for preliminary NMR measurements, Mrs. Dominique Melck (Istituto di Chimica Biomolecolare del CNR) for technical assistance with NMR experiments, Mr. Emilio P. Castelluccio for computer system maintenance, and Prof. Orlando Crescenzi (Università di Napoli Federico II, Naples, Italy) for helpful discussions. We are grateful to the anonymous referees for many constructive criticisms.

REFERENCES

- Wright, P. E., and Dyson, H. J. (1999) Intrinsically unstructured proteins: Re-assessing the protein structure-function paradigm, *J. Mol. Biol.* 293, 321–331.
- Tomba, P. (2002) Intrinsically unstructured proteins, *Trends Biochem. Sci.* 27, 527–533.
- Smith, L. J., Bolin, K. A., Schwalbe, H., MacArthur, M. W., Thornton, J. M., and Dobson, C. M. (1996) Analysis of main chain torsion angles in proteins: Prediction of NMR coupling constants for native and random coil conformations, *J. Mol. Biol.* 255, 494–506.
- Dyson, H. J., Rance, M., Houghten, R. A., Lerner, R. A., and Wright, P. E. (1988) Folding of immunogenic peptide fragments of proteins in water solution. I. Sequence requirements for the formation of a reverse turn, *J. Mol. Biol.* 201, 161–200.
- Shi, Z., Woody, R. W., and Kallenbach, N. R. (2002) Is polyproline II a major backbone conformation in unfolded proteins? *Adv. Protein Chem.* 62, 163–240.
- Eker, F., Cao, X., Nafie, L., Huang, Q., and Schweitzer-Stenner, R. (2003) The structure of alanine based tripeptides in water and dimethyl sulfoxide probed by vibrational Spectroscopy, *J. Phys. Chem. B* 107, 358–365.
- Pappu, R. V., and Rose, G. D. (2002) A simple model for polyproline II structure in unfolded states of alanine-based peptides, *Protein Sci.* 11, 2437–2455.
- Park, S.-H., Shalongo, W., and Stellwagen, E. (1997) The role of PII conformations in the calculation of peptide fractional helix content, *Protein Sci.* 6, 1694–1700.
- Shi, Z., Olson, C. A., Rose, G. D., Baldwin, R. L., and Kallenbach, N. R. (2002) Polyproline II structure in a sequence of seven alanine residues, *Proc. Natl. Acad. Sci. U.S.A.* 99, 9190–9195.
- Weise, C. F., and Weisshaar, J. C. (2003) Conformational analysis of alanine dipeptide from dipolar couplings in a water-based liquid crystal, *J. Phys. Chem. B* 107, 3265–3277.
- Eker, F., Griebenow, K., and Schweitzer-Stenner, R. (2003) Stable conformations of tripeptides in aqueous solution studied by UV circular dichroism spectroscopy, *J. Am. Chem. Soc.* 125, 8178–8185.
- Gazit, E. (2002) A possible role for π -stacking in the self-assembly of amyloid fibrils, *FASEB J.* 16, 77–83.

13. Reches, M., and Gazit, E. (2003) Casting metal nanowires within discrete self-assembled peptide nanotubes, *Science* 300, 625–627.
14. Reches, M., and Gazit, E. (2004) Amyloidogenic Hexapeptide Fragment of Medin: Implications for the Stacking Model of Fibrillization, *Amyloid* 11, 81–89.
15. Yang, D., Li, W., Qu, J., Luo, S.-W., and Wu, Y.-D. (2003) A new strategy to induce γ -turns: Peptides composed of alternating α -aminoxy acids and α -amino acids, *J. Am. Chem. Soc.* 125, 13018–13019.
16. Eker, F., Griebenow, K., Cao, X., Nafie, L. A., and Schweitzer-Stenner, R. (2004) Preferred peptide backbone conformations in the unfolded state revealed by the structure analysis of alanine-based (AXA) tripeptides in aqueous solution, *Proc. Natl. Acad. Sci. U.S.A.* 101, 10054–10059.
17. Némethy, G., and Printz, M. P. (1972) The γ -turn, a possible folded conformation of the polypeptide chain. Comparison with the β -turn, *Macromolecules* 5, 755–758.
18. Milner-White, E. J. (1990) Situations of γ -turns in proteins. Their relation to α -helices, β -sheets and ligand binding sites, *J. Mol. Biol.* 216, 386–397.
19. Schmidt, J. M., Ohlenschläger, O., Rüterjans, H., Grzonka, Z., Kojro, E., Pavo, I., and Fahrenholz, F. (1991) Conformation of [8-arginine]vasopressin and V1 antagonists in dimethyl sulfoxide solution derived from two-dimensional NMR spectroscopy and molecular dynamics simulation, *Eur. J. Biochem.* 201, 355–371.
20. Walse, B., Kihlberg, J., and Drakenberg, T. (1998) Conformation of desmopressin, an analogue of the peptide hormone vasopressin, in aqueous solution as determined by NMR spectroscopy, *Eur. J. Biochem.* 252, 428–440.
21. Sato, M., Lee, J. Y. H., Nakanishi, H., Johnson, M. E., Chrusciel, R. A., and Kahn, M. (1992) Design, synthesis and conformational analysis of γ -turn peptide mimetics of bradykinin, *Biochem. Biophys. Res. Commun.* 187, 999–1006.
22. Schmidt, B., Lindman, S., Tong, W., Lindeberg, G., Gogoll, A., Lai, Z., Thörnwall, M., Synnergren, B., Nilsson, A., Welch, C. J., Sohtell, M., Westerlund, C., Nyberg, F., Karlén, A., and Hallberg, A. (1997) Design, synthesis, and biological activities of four angiotensin II receptor ligands with γ -turn mimetics replacing amino acid residues 3–5, *J. Med. Chem.* 40, 903–919.
23. Haubner, R., Gratias, R., Diefenbach, B., Goodman, S. L., Jonczyk, A., and Kessler, H. (1996) Structural and functional aspects of RGD-containing cyclic pentapeptides as highly potent and selective integrin $\alpha_5\beta_3$ antagonists, *J. Am. Chem. Soc.* 118, 7461–7472.
24. Schumann, F., Müller, A., Koksche, M., Müller, G., and Sewald, N. (2000) Are β -amino acids γ -turn mimetics? Exploring a new design principle for bioactive cyclopeptides, *J. Am. Chem. Soc.* 122, 12009–12010.
25. Barron, L. D., Hecht, L., Blanch, E. W., and Bell, A. F. (2000) Solution structure and dynamics of biomolecules from Raman optical activity, *Prog. Biophys. Mol. Biol.* 73, 1–49.
26. States, D. J., Haberkorn, R. A., and Ruben, D. J. (1982) A two-dimensional nuclear Overhauser experiment with pure absorption phase in four quadrants, *J. Magn. Reson.* 48, 286–292.
27. Griesinger, C., Otting, G., Wüthrich, K., and Ernst, R. R. (1988) Clean TOCSY for H-1 spin system-identification in macromolecules, *J. Am. Chem. Soc.* 110, 7870–7872.
28. Bothner-By, A. A., Stephens, R. L., Lee, J. M., Warren, C. D., and Jeanloz, R. W. (1984) Structure determination of a tetrasaccharide: Transient nuclear Overhauser effects in the rotating frame, *J. Am. Chem. Soc.* 106, 811–813.
29. Hwang, T.-L., and Shaka, A. J. (1995) Water suppression that works: Excitation sculpting using arbitrary wave-forms and pulsed-field gradient, *J. Magn. Reson.* 112, 275–279.
30. Bodenhausen, G., and Ruben, D. J. (1980) Natural abundance nitrogen-15 NMR by enhanced heteronuclear spectroscopy, *Chem. Phys. Lett.* 69, 185–189.
31. Neuhaus, D., Wagner, G., Vasák, M., Kägi, J. H. R., and Wüthrich, K. (1985) Systematic application of high-resolution, phase-sensitive two-dimensional ^1H NMR techniques for the identification of the amino acid-proton spin systems in proteins. Rabbit metallothionein-2, *Eur. J. Biochem.* 151, 257–273.
32. Neuhaus, D., and Williamson, M. (1989) *The nuclear Overhauser effect in structural and conformational analysis*, VCH Publishers, New York.
33. Güntert, P., Braun, W., Billeter, M., and Wüthrich, K. (1989) Automated stereospecific proton NMR assignments and their impact on the precision of protein structure determinations in solution, *J. Am. Chem. Soc.* 111, 3997–4004.
34. Koning, T. M. G., Boelens, R., and Kaptein, R. (1990) Calculation of the nuclear Overhauser effect and the determination of proton–proton distances in the presence of internal motions, *J. Magn. Reson.* 90, 111–123.
35. Güntert, P. (2004) Automated NMR structure calculation with CYANA, *Methods Mol. Biol.* 278, 353–378.
36. van Gunsteren, W. F., and Berendsen, H. J. C. (1987) *Groningen Molecular Simulation (GROMOS) Library Manual*, pp 1–229, BIOMOS, Groningen, The Netherlands.
37. Ryckaert, J. P., Ciccotti, G., and Berendsen, H. J. C. (1977) Numerical integration of the Cartesian equations of motions of a system with constraints: Molecular dynamics of *n*-alkanes, *J. Comput. Phys.* 23, 327–341.
38. van Gunsteren, W. F., and Berendsen, H. J. C. (1977) Algorithms for macromolecular dynamics and constraint dynamics, *Mol. Phys.* 34, 1311–1327.
39. Koradi, R., Billeter, M., and Wüthrich, K. (1996) MOLMOL: A program for display and analysis of macromolecular structures, *J. Mol. Graphics* 14, 51–55.
40. Weiner, S. J., Kollman, P. A., Case, D. A., Singh, U. C., Ghio, C., Alagona, G., Profeta, S., and Weiner, P. (1984) A new force field for molecular mechanical simulation of nucleic acids and proteins, *J. Am. Chem. Soc.* 106, 765–784.
41. Weiner, S. J., Kollman, P. A., Nguyen, D. T., and Case, D. A. (1986) An all-atom force-field for simulations of proteins and nucleic acids, *J. Comput. Chem.* 7, 230–252.
42. Press, W. A., Flannery, B. P., Teukolsky, S. A., and Vetterling, W. T. (1986) *Numerical Recipes: The Art of Scientific Computing*, pp 307–312, Columbia University Press, Cambridge, U.K.
43. Johnson, W. C., Jr. (1988) Secondary structure of proteins through circular dichroism spectroscopy, *Annu. Rev. Biophys. Biophys. Chem.* 17, 145–166.
44. Shaw, R. A., Perczel, A., Mantsch, H. H., and Fasman, G. D. (1994) Turns in small cyclic peptides: Can infrared spectroscopy detect and discriminate amongst them? *J. Mol. Struct.* 324, 143–150.
45. Vass, E., Hollosi, M., Besson, F., and Buchet, R. (2003) Vibrational spectroscopic detection of β - and γ -turns in synthetic and natural peptides and proteins, *Chem. Rev.* 103, 1917–1954.
46. Wüthrich, K. (1986) *NMR of Proteins and Nucleic Acids*, Wiley, New York.
47. Wishart, D. S., and Sykes, B. D. (1994) Chemical shifts as a tool for structure determination, *Methods Enzymol.* 239, 363–392.
48. Bundi, A., and Wüthrich, K. (1979) ^1H NMR parameters of the common amino acid residues measured in aqueous solution of linear tetrapeptides Gly-Gly-X-Ala, *Biopolymers* 18, 299–311.
49. de Alba, E., Blanco, F. J., Jiménez, M. A., Rico, M., and Nieto, J. L. (1995) Interactions responsible for the pH dependence of the β -hairpin conformational population formed by a designed linear peptide, *Eur. J. Biochem.* 233, 283–292.
50. Schwarzing, S., Kroon, G. J., Foss, T. R., Chung, J., Wright, P. E., and Dyson, H. J. (2001) Sequence-dependent correction of random coil NMR chemical shifts, *J. Am. Chem. Soc.* 123, 2970–2978.
51. Eker, F., Cao, X., Nafie, L., and Schweitzer-Stenner, R. (2002) Tripeptides adopt stable structures in water. A combined polarized visible Raman, FTIR, and VCD spectroscopy study, *J. Am. Chem. Soc.* 124, 14330–14341.
52. Guruprasad, K., and Rajkumar, S. (2000) β - and γ -turns in proteins revisited: A new set of amino acid turn-type dependent positional preferences and potentials, *J. Biosci.* 25, 143–156.
53. de Alba, E., Jimenez, M. A., Rico, M., and Nieto, J. L. (1996) Conformational investigation of designed short linear peptides able to fold into β -hairpin structures in aqueous solution, *Folding Des.* 1, 133–144.
54. Flory, P. J. (1969) *Statistical Mechanics of Chain Molecules*, pp 30–31, Wiley, New York.
55. Santiveri, C. M., Rico, M., and Jimenez, M. A. (2001) $^{13}\text{C}_\alpha$ and $^{13}\text{C}_\beta$ chemical shifts as a tool to delineate β -hairpin structures in peptides, *J. Biomol. NMR* 19, 331–345.
56. Amodeo, P., Motta, A., Tancredi, T., Salvatori, S., Tomatis, R., Saviano, G., and Temussi, P. A. (1992) Solution structure of deltorphin I at 265 K: A quantitative NMR study, *Pept. Res.* 5, 48–55.
57. Schweitzer-Stenner, R., Eker, F., Huang, Q., and Griebenow, K. (2001) Dihedral angles of trialanine in D_2O determined by combining FTIR and polarized visible Raman spectroscopy, *J. Am. Chem. Soc.* 123, 9628–9633.

58. Sundaralingam, M., and Sekharudu, Y. C. (1989) Water-inserted α -helical segments implicate reverse turns as folding intermediates, *Science* **244**, 1333–1337.
59. Zimmerman, S. S., and Scheraga, H. A. (1977) Local interactions in bends of proteins, *Proc. Natl. Acad. Sci. U.S.A.* **74**, 4126–4129.
60. Wright, P. E., Dyson, H. J., and Lerner, R. A. (1988) Conformation of peptide fragments of proteins in aqueous solution: Implications for initiation of protein folding, *Biochemistry* **27**, 7167–7165.
61. Yu, M. H., and King, J. (1988) Surface amino acids as sites of temperature-sensitive folding mutations in the P22 tailspike protein, *J. Biol. Chem.* **263**, 1424–1431.
62. Kiso, Y., Matsumoto, H., Mizumoto, S., Kimura, T., Fujiwara, Y., and Akaji, K. (1999) Small dipeptide-based HIV protease inhibitors containing the hydroxymethylcarbonyl isostere as an ideal transition-state mimic, *Biopolymers* **51**, 59–68.
63. Goodman, M., Zhu, Q., Kent, D. R., Amino, Y., Iacovino, R., Benedetti, E., and Santini, A. (1997) Conformational analysis of the dipeptide taste ligand L-aspartyl-D-2-aminobutyric acid-(S)- α -ethylbenzylamide and its analogues by NMR spectroscopy, computer simulations and X-ray diffraction studies, *J. Pept. Sci.* **3**, 231–241.
64. Torreggiani, A., Tamba, M., and Fini, G. (2000) Binding of copper(II) to carnosine: Raman and IR spectroscopic study, *Biopolymers* **57**, 149–159.
65. Sato, M., Lee, J. Y., Nakanishi, H., Johnson, M. E., Chrusciel, R. A., and Kahn, M. (1992) Design, synthesis and conformational analysis of γ -turn peptide mimetics of bradykinin, *Biochem. Biophys. Res. Commun.* **187**, 999–1006.
66. Yuan, Z., Blomberg, D., Sethson, I., Brickmann, K., Ekholm, K., Johansson, B., Nilsson, A., and Kihlberg, J. (2002) Synthesis and pharmacological evaluation of an analogue of the peptide hormone oxytocin that contains a mimetic of an inverse γ -turn, *J. Med. Chem.* **45**, 2512–2519.
67. Romano, R., Esposito, R., Indovina, P. L., Barone, F., and Motta, A. (2005) CAKE: A Monte Carlo approach to fractional volume integration in two-dimensional NMR spectroscopy, *J. Biomol. NMR* (submitted for publication).
68. Hyberts, S. G., Goldberg, M. S., Havel, T. F., and Wagner, G. (1992) *Protein Sci.* **1**, 736–751.

BI050658V